Accepted manuscript. To appear in Proc. IEEE OCEANS 2026, Monterey, CA, USA.
© 2026 IEEE. Personal use of this material is permitted. Permission from IEEE must be obtained for all other uses, in any current or future media, including reprinting/republishing this material for advertising or promotional purposes, creating new collective works, for resale or redistribution to servers or lists, or reuse of any copyrighted component of this work in other works.

A Tethered Multi-UUV Architecture for Cooperative Sensing and Interception of Underwater Threats

Anurag Koyyada
Cornell University
Ithaca, USA

Wesley Dalton
University of Pennsylvania
Philadelphia, USA

Alex Rice
Georgia Institute of Technology
Atlanta, USA

Joel Santiago-Baretti
Massachusetts Institute of Technology
Cambridge, USA

Gregory Falco
Cornell University
Ithaca, USA

***Abstract*—The proliferation of low-cost uncrewed underwater vehicles (UUVs) poses an asymmetric defense problem for critical maritime infrastructure, ports, naval vessels, and high-value nearshore structures. Contemporary maritime defense architectures remain weighted toward situational awareness, with limited capability to deny or neutralize threats once detected.**

We present KRAKEN, a cooperative multi-UUV architecture for the cooperative sensing and interception of underwater threats. Sensor-laden tethered UUVs are deployed to localize inbound targets, a central processing node fuses their observations, and a payload-carrying tethered UUV is continuously directed along the dynamic track until interdiction. A prototype tethered UUV was built to validate component integration, bench tether communications, and fly-by-wire control.

We conducted a 40,700-trial Monte Carlo campaign using a reduced-order model incorporating sonar detection, navigation uncertainty, communications latency, interceptor kinematics, tether drag, and multi-vehicle cable interference to evaluate the architecture against autonomous single-interceptor and acoustic-communications alternatives. First, cooperative target tracking is found to substantially reduce sensitivity to initial cue error: the fused-scout architecture maintains capture probability $P_cap \geq 0.987$ through 10° of cue-bearing error and $P_cap = 0.860$ at 20°, while a cue-fired interceptor using its own onboard sensors degrades sharply as cue uncertainty increases. Second, low-latency communications are critical for reliable closed-loop interception. With three scouts and a 3.0 m/s threat, the modeled fiber architecture achieves $P_cap = 1.000$, compared with $P_cap = 0.375$ for the best case acoustic link. Third, tether configuration strongly affects interception performance. Vehicle-side payout of a 0.9 mm fiber link maintains $P_cap \geq 0.96$ through 4 m/s for straight inbound threats, whereas UUV-towed configurations incur significant hydrodynamic drag and risk cable-clearance failures. The results suggest that cooperative interdiction of underwater threats depends not only on interceptor speed or onboard autonomy, but on the interaction between cooperative localization, engagement geometry, and tether configuration.

***Index Terms*—Counter-UUV, maritime defense, cooperative localization, tethered vehicles, marine security**

I. Introduction

As low-cost uncrewed underwater vehicles (UUVs) proliferate—posing asymmetric threats to critical maritime infrastructure, ports, naval vessels, and high-value nearshore structures—response mechanisms are insufficient for maritime security. Despite advances in underwater sensing, detection, tracking and classification, today's architectures lack robust means for interdiction and denial. This gap is particularly acute in contested and communication-denied environments, where human-in-the-loop responses are delayed or infeasible.

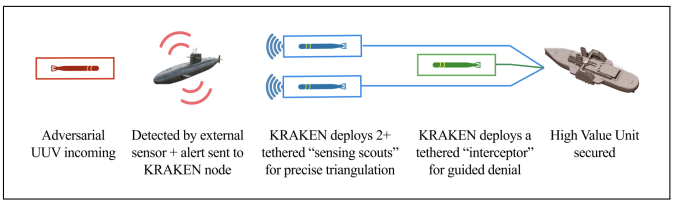


Fig. 1. Overview of KRAKEN architecture.

First, we introduce KRAKEN, a multi-UUV architecture for cooperative real-time underwater defense and threat interdiction under communication constraints. KRAKEN integrates distributed heterogeneous sensing, centralized track fusion, and coordinated deployment of tethered threat-sensing and -intercepting UUVs. Second, we develop an analytical and simulation-based framework that jointly models sonar detection, navigation uncertainty, communications latency, interceptor kinematics, tether drag, and multi-vehicle cable interference. Third, we evaluate the architecture through a frozen 40,700-trial Monte Carlo campaign and quantify how sensing geometry, communications architecture, navigation quality, and tether configuration affect interception probability.

Operationally, an external cue triggers deployment of tethered sensor-laden UUVs to flank inbound submersible threats and reduce engagement uncertainty via localized sensing and sonar-based triangulation. Each UUV produces local range-bearing observations that a central processing node fuses with vehicle-position estimates to form and continuously maintain a target track. Once classification, localization, and kinematic launch conditions are satisfied, the node dispatches a tethered payload-carrying interceptor and guides it to interdiction. Fiber-optic tethers transport command, telemetry, and sensor data between the central node and all UUVs without the propagation and shared-medium penalties of underwater acoustic communications.

II. Related Work

KRAKEN builds on work in harbor surveillance and defense, cooperative underwater localization and tracking, tethered-vehicle mechanics, and underwater communications. Although researchers have established the viability of tethered UUVs for ship hull maintenance [1], deep-water scientific exploration [2]–[4], minesweeping [5], and military payload delivery [6], cooperative multi-UUV architectures for underwater threat denial have received little attention. Given the critical role of maritime infrastructure (e.g., submarine cables) for global security, telecommunications, financial systems, and beyond, marine defense is increasingly a priority concern [7].

Harbor protection architectures have long integrated sonar-based detection, classification, tracking, decision support, and counter-UUV response, while MIMO-sonar methods have addressed recognition and tracking of low-profile targets in cluttered harbor environments [8], [9]. Following, active-response work has considered coordinated USV interception of detected threats and multi-AUV interception using predicted target motion and path planning [10], [11]. More recent multi-AUV defense work formulates three-dimensional many-versus-many attack–defense problems and coordinates defending vehicles through hierarchical multi-agent reinforcement learning [12]. Whereas these studies primarily address response after a threat has been detected or localized sufficiently for interceptor assignment or trajectory planning, KRAKEN instead evaluates how uncertainty introduced at the cueing-stage propagates through cooperative localization, fused track formation, communications-dependent guidance, and tether-constrained interception to affect engagement outcomes.

Cooperative localization and target tracking provide the estimation basis for this architecture. Multi-AUV systems have already demonstrated cooperative positioning using inter-vehicle acoustic ranging and exchanged navigation information, while Fisher-information and Cramér–Rao analyses establish the dependence of range-based localization accuracy on sensor geometry [13], [14]. Recent approaches jointly address cooperative localization and target tracking in anchor-free environments by exploiting environmental-current information as an additional reference [15]. Heterogeneous UAV–USV–UUV networks have further coupled cooperative detection geometry, underwater target tracking, and communication connectivity constraints [16]. Meanwhile, KRAKEN does not introduce a new localization or tracking algorithm, but propagates scout-pose and sonar-measurement uncertainty into a fused interception track and evaluates how sensor geometry, scout count, and navigation quality affect subsequent interception probability.

Tethered vehicles introduce direct coupling between communications architecture and vehicle dynamics. Cable forces can materially alter underwater-vehicle motion, and coupled ROV–umbilical models demonstrate nonlinear interactions among vehicle dynamics, hydrodynamic loading, and deployed cable geometry [17], [18]. Lightweight optical-fiber systems provide a mechanically distinct regime in which low-tension fiber can be paid out behind a moving vehicle rather than continuously towing the full deployed length through the water [19]. KRAKEN incorporates these regimes by treating host-spooled and vehicle-spooled tethers as distinct mechanical architectures and evaluating both hydrodynamic performance and inter-vehicle cable-clearance constraints.

Underwater acoustic communications are constrained by low propagation velocity, range- and frequency-dependent bandwidth, extended multipath, and Doppler effects [20], [21]. At the MAC layer, long propagation delays and shared-channel access have motivated specialized protocols such as Slotted FAMA, T-Lohi, and STUMP which mitigate these constraints through propagation-aware contention and scheduling [22]–[24]. KRAKEN does not propose a new acoustic MAC or treat equal-share TDMA as a fundamental channel limit. Instead, it uses a conservative shared-medium acoustic baseline and carries update rate, packet loss, propagation delay, and resulting state age into target fusion and interceptor guidance.

III. System Architecture

KRAKEN is a cooperative multi-UUV sensing and interception architecture in which a central processing node colocated with, or nearby, a defended asset deploys tethered sensor-laden UUVs ("scouts"), fuses their observations, and guides a tethered payload-carrying interceptor UUV towards inbound underwater threats. Triggered by external sensors, scouts are deployed in a fan about the cue direction and obtain active-sonar range–bearing measurements. The baseline assumes USBL-supported navigation, while dedicated fiber links carry command, telemetry, and sensor data between the deployed vehicles and the host.

Scout reports are fused at the central processing node using a constant-velocity EKF that accounts for reported measurement uncertainty and scout-pose covariance. A confirmed track is classified as hostile using a windowed kinematic classifier. Interceptor launch requires a hostile track, horizontal track uncertainty below the launch gate, and a feasible kinematic rollout subject to tether and deconfliction constraints. After launch, the interceptor is guided until geometric capture or a terminal failure condition is reached.

Two architectural choices are central to the evaluation. First, sensing is distributed but decision-making is centralized: scouts provide observations, while the central node ("host") maintains the fused track and commands interceptor launch and midcourse guidance. Second, the baseline uses vehicle-spooled 0.9 mm fiber. Unlike host-spooled cable, which is continuously towed through the water, vehicle-side payout leaves most deployed cable behind the vehicle and therefore reduces both hydrodynamic drag and cable-interference risk.

The baseline configuration uses three scouts, a 60 kHz FM multibeam sonar, USBL-supported navigation, fiber command and telemetry, and a vehicle-spooled interceptor tether; remaining simulation parameters are summarized in Table I. Results compare this architecture against two alternatives: a cue-fired autonomous interceptor carrying its own 120 kHz seeker, and an otherwise cooperative fleet using a shared acoustic link in place of dedicated fiber.

TABLE I
BASELINE SIMULATION PARAMETERS.

Environment	
water depth	12 m
far-field spreading exponent	15
ambient noise spectral level	75 dB
bottom backscatter strength	-27 dB
Sonar	
frequency	60 kHz
source level	200 dB
pulse length	0.20 ms
per-beam width	2.5 deg
sector width	120 deg
target strength	-15 dB
per-cell P_{fa}	10^{-7}
ping interval	0.67 s
Vehicle	
thrust	49 N
free-stream speed	4.99 m/s
lateral acceleration limit	2.0 m/s^2
minimum turn radius	12.4 m
Engagement	
cue range	400 m
cue bearing error	10 deg
scout standoff	120 m
launch gate	$\sigma_h \leq 15$ m
capture radius	5 m
control step	0.2 s

IV. HARDWARE PROTOTYPING AND VALIDATION POSTURE

A prototype tethered UUV was constructed to validate vehicle integration, bench tether communications, and fly-by-wire control. The 0.6 m vehicle uses a PVC hull, an ApisQueen U2 thruster powered by a 6S LiPo battery, three servo-actuated control surfaces, a Pixhawk running ArduSub, and a Raspberry Pi companion computer. The companion bridges tethered Ethernet to the autopilot over MAVLink and provides an interface for future sensing and interdiction payloads. Table II distinguishes the as-built prototype from the reference design used in the system evaluation.

The reference design replaces the prototype's bench-length copper Ethernet tether with single-mode fiber while retaining onboard vehicle power. Fiber is used as the baseline command and telemetry link because its modeled propagation and conversion delays are negligible relative to the guidance update interval. Acoustic communications, which introduce propagation delay, packet loss, and shared-medium constraints, are evaluated separately as a degraded alternative.

Absolute navigation is not integrated. The reference design assumes onboard inertial and depth sensing supplemented by a surveyed USBL system at the control station, with position fixes returned over fiber link. Horizontal position uncertainty is modeled as range dependent and is propagated into the scout-pose covariance used by the target-tracking filter.

The prototype demonstrates mechanical and electronic integration, tethered bench communications, and fly-by-wire actuation, but does not validate the fiber, USBL, sonar, or interdiction subsystems in water. Fiber-linked navigation, sensing, and in-water closed-loop validation is left for future work.

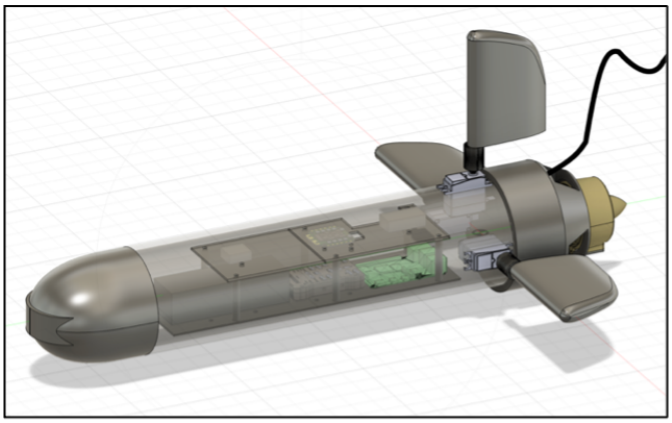


Fig. 2. As-built COTS tethered UUV prototype, demonstrating component integration and body form.

TABLE II
AS-BUILT PROTOTYPE VERSUS REFERENCE DESIGN.

Subsystem	**As-built**	**Reference design**	**Status**
Structure	4 in PVC, 0.6 m	Pressure-rated composite hull	Built
Tether	Copper Ethernet, bench length	Single-mode fiber, rotary joint	Specified
Autopilot	Pixhawk, ArduSub	Unchanged	Built
Companion	Raspberry Pi	Unchanged	Built
Propulsion	ApisQueen U2, ESC, 6S LiPo	Unchanged	Built
Actuation	Three servo surfaces	Unchanged	Built
Absolute nav	None	USBL beacon, depth, ext. compass	Specified
Payload sens.	None	Sonar head	Not built
Interdiction	None	Net or kinetic module	Not built

V. MODELS AND SIMULATION

A. Acoustic Detection

Active sonar is modeled as reverberation limited. Propagation uses spherical spreading at short range and an environment-dependent spreading exponent beyond the depth transition; absorption follows Thorp [25]. Reverberation and ambient noise are combined incoherently following the active-sonar model [26]. Detection probability is evaluated using the nonfluctuating-target Marcum-Q formulation [27], [28] at the specified per-cell false-alarm probability. Measurement uncertainty follows Cramér–Rao scaling with calibration floors in range and bearing. Scout ping intervals are limited by two-way acoustic travel time; scouts ping independently, corresponding to a fiber-backed, separated-band or staggered-ping CONOPS.

B. Navigation and Tracking

Each scout carries a believed pose whose uncertainty is propagated into its target measurements. The USBL navigation model includes range-dependent position error, while dead-reckoning error is separated into deployment bias and

update noise. Localization geometry is characterized using the horizontal position Cramér–Rao bound for range–bearing–elevation measurements, including sensor-pose covariance [29].

Target reports are fused using a constant-velocity Cartesian EKF. The measurement covariance supplied to the filter incorporates sonar measurement uncertainty and scout-pose uncertainty, allowing navigation quality and scout geometry to propagate directly into the fused track used for interceptor guidance.

C. Tether Mechanics and Cable Geometry

Vehicle speed is determined from a steady force balance between available thrust, hull drag, and tether drag. The effective moving cable length is the full deployed length for a host-spooled tether but only a short dispenser segment for vehicle-side payout. Consequently, host-spooled cable increasingly limits achievable speed with deployed length, whereas vehicle-spooled 0.9 mm fiber retains substantially more of the vehicle's free-stream capability (Fig. 3).

Cable interference is evaluated geometrically. Host-spooled cables are represented as straight segments from fairlead to vehicle, whereas vehicle-spooled fiber is laid along the vehicle trajectory. A foul is scored when two modeled cable bodies approach within a prescribed clearance envelope, nominally $d_{\mathrm{clear}} = 1$ m, representing uncertainty from sag, current, and pose error rather than physical cable diameter.

D. Communications and Engagement Dynamics

The cooperative architecture contains a scout-to-host contact uplink and a host-to-interceptor fused-state downlink. Fiber links are modeled as dedicated channels with propagation near 2×10^8 m/s, 5 ms processing delay, and 10^{-4} packet loss. Acoustic alternatives include sound-speed propagation, packet loss, jitter, and shared-channel TDMA, causing per-node update rate to decrease with the number of sharing vehicles [20]. Received target states are extrapolated according to their communication age; beyond a maximum allowable state age, the guidance picture is declared lost.

Vehicles are modeled as rate-limited planar unicycles subject to tether-dependent speed ceilings and lateral-acceleration limits. The baseline interceptor uses vector proportional navigation with navigation constant $N = 4$ and a filtered line-of-sight rate [30]; pure pursuit, line-of-sight path following, and a predicted-intercept-point waypoint are included in the endgame sweep. Capture is determined from the exact minimum relative separation along each simulation-step line segment rather than from endpoint sampling. These reduced-order models omit full six-degree-of-freedom vehicle dynamics; their implications are discussed in Section VIII.

VI. Monte Carlo Method

Each Monte Carlo trial represents one engagement and is classified as captured or by failure mode: missed, leaker, entangled, never detected, never hostile, launch gate not met, intercept infeasible, guidance picture lost, tether exhausted, or timeout. Capture is scored when the swept closest point of approach satisfies CPA $\leq R$, with $R = 5$ m, unless a cable foul occurs at or before closest approach. Nine parameter sweeps comprise the frozen campaign of 40,700 independent trials (Table III). Deterministic seeding is used for reproducibility, and Wilson 95% confidence intervals are reported for capture probability P_cap [31]. Miss-distance quantiles are computed over captured and missed engagements only.

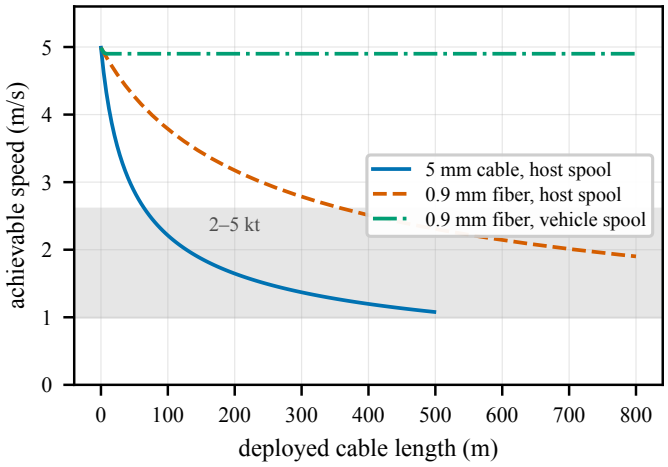


Fig. 3. Achievable interceptor speed versus deployed cable length for host-spooled and vehicle-spooled cables.

TABLE III
Frozen Monte Carlo campaign (40,700 independent trials).

Sweep	n	Primary factors
Baseline	500	Recommended CONOPS
Geometry	5760	Fan width, scout count, sensor
Navigation	2400	Pose-error model, scout count
Comms	4800	Link, scout count, threat speed
Autonomy	3000	Cooperative vs. seeker, cue error
Entanglement	7200	Spool, scouts, depth, corridor
Envelope	7200	Speed, maneuver, cable
Sensing	3840	Sonar, environment, target strength
Endgame	6000	Acceleration, guidance law, launch gate

VII. Results

A. Sensing Geometry and Navigation

The 60 kHz multibeam provides the most useful baseline sensing performance in the modeled busy-harbor environment. As summarized in Table IV, the 750 kHz short-range sonar is ineffective at engagement-scale ranges, while the 60 kHz CW alternative exhibits strong aspect dependence. The 60 kHz FM multibeam therefore provides the most consistent engagement-scale coverage across closing and crossing geometries.

With the baseline multibeam, separated multi-scout geometries generally achieve high capture probability, whereas colocating multiple tethered scouts on the same bearing produces systematic cable fouling (Fig. 4a).

Navigation quality determines when additional scouts provide useful estimation gain (Fig. 4b). Under USBL-supported navigation, capture probability is already near saturation at

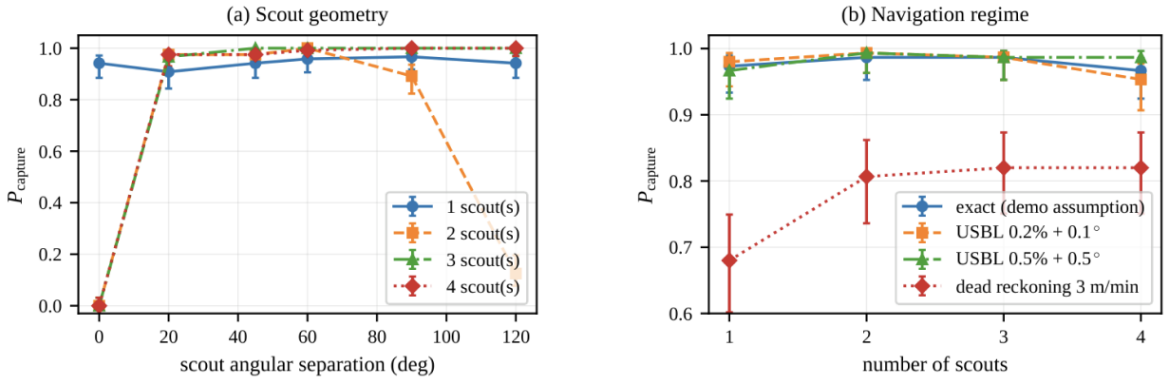


Fig. 4. Effects of scout geometry and navigation quality on cooperative interception performance: (a) capture probability versus scout angular separation for the baseline 60 kHz FM multibeam; (b) capture probability versus scout count under different navigation regimes.

TABLE IV
MODELED $P_d = 0.5$ DETECTION RANGE IN THE BUSY-HARBOR ENVIRONMENT FOR A -15 DB TARGET-STRENGTH UUV.

Sensor	R_{50} **Closing (m)**	R_{50} **Crossing (m)**
750 kHz Ping360	18	18
60 kHz FM multibeam	85	85
60 kHz CW multibeam	287	11
20 kHz low-frequency	27	27

$N = 1$–2; increasing scout count from one to four changes P_{cap} only from 0.967 to 0.987. Under free dead reckoning, increasing scout count from one to four raises P_{cap} from 0.680 to 0.820 while reducing median track error from 4.07 m to 3.04 m. These results motivate the three-scout baseline as a compromise between localization robustness and cable-management complexity.

B. Cue Robustness and Communications

Cooperative sensing substantially reduces sensitivity to initial cue uncertainty (Fig. 5). The cue-fired autonomous interceptor degrades rapidly as bearing uncertainty increases, with $P_cap = 0.517$ at 5° and 0.287 at 10°. In contrast, the cooperative architecture maintains $P_cap \geq 0.987$ through 10° cue-bearing error and achieves $P_cap = 0.860$ at 20°. Cooperative median miss distance remains approximately 0.9 m across the cue-error sweep.

Low-latency communications are likewise critical to closed-loop interception. With three scouts, fiber achieves $P_cap = 0.992$ at 1.5 m/s and 1.000 at 3.0 m/s, compared with 0.925 and 0.375, respectively, for the best modeled acoustic link (Table V). Mean guidance-state age is 0.10 s on fiber and approximately 3.2 s on acoustic-good, while the per-scout update rate falls from 10 Hz to 0.33 Hz. Degraded, denied, and absent cooperative links yield no capture in evaluated cells.

C. Tether Configuration and Engagement Envelope

Tether architecture produces a first-order change in interception performance (Fig. 6). For a straight 2 m/s threat, vehicle-spooled 0.9 mm fiber achieves $P_cap = 0.99$ with no modeled cable fouls, compared with $P_cap = 0.54$ for the same fiber

TABLE V
THREE-SCOUT CAPTURE PROBABILITY, UPLINK RATE, AND GUIDANCE-STATE AGE BY LINK REGIME AND THREAT SPEED.

Link	Rate (Hz)	Age (s)	P_{cap}	95% CI	Miss p_{50} (m)
fiber (1.5 m/s)	10.00	0.10	0.99	[0.95, 1.00]	1.1
fiber (3 m/s)	10.00	0.10	1.00	[0.97, 1.00]	0.9
acoustic good (1.5 m/s)	0.33	3.22	0.93	[0.86, 0.96]	1.9
acoustic good (3 m/s)	0.33	3.20	0.38	[0.29, 0.46]	2.6
acoustic degraded (1.5 m/s)	0.12	—	0.00	[0.00, 0.03]	—
acoustic degraded (3 m/s)	0.12	—	0.00	[0.00, 0.03]	—
acoustic denied (1.5 m/s)	0.08	—	0.00	[0.00, 0.03]	—
acoustic denied (3 m/s)	0.08	—	0.00	[0.00, 0.03]	—
none (1.5 m/s)	0.00	—	0.00	[0.00, 0.03]	—
none (3 m/s)	0.00	—	0.00	[0.00, 0.03]	—

towed from the host and $P_cap = 0.48$ for a 5 mm host-spooled cable. With vehicle-side payout, straight-threat capture probability remains at or above 0.96 through 4 m/s and falls to 0.48 at 5 m/s. Weaving threats remain at $P_cap \geq 0.89$ through 4 m/s, whereas the scripted evasive policy reduces capture probability to 0.05 or less at 1.5 m/s and above.

Cable deconfliction further supports the three-scout baseline. For three scouts, launch-corridor deconfliction reduces modeled cable-foul probability from 0.07 to 0.01 and raises P_{cap} from 0.93 to 0.99; combining corridor and depth separation eliminates modeled fouling and yields $P_{cap} = 1.00$.

The recommended configuration, evaluated over 500 trials, yields a capture fraction of 0.990, with leaker, entangled, and missed fractions of 0.006, 0.002, and 0.002, respectively. Median launch and capture times are 103 s and 133 s.

VIII. LIMITATIONS

The results should be interpreted within the fidelity of the reduced-order models used here. Vehicle motion is represented by rate-limited planar unicycles with tether-dependent speed and turn constraints rather than full six-degree-of-freedom hydrodynamics, and the headline sweeps are effectively still-water cases. The acoustic model likewise uses a simplified environment without a spatially varying sound-speed profile and represents bottom interaction through a single backscatter parameter. Cable fouling is modeled geometrically using a 1 m

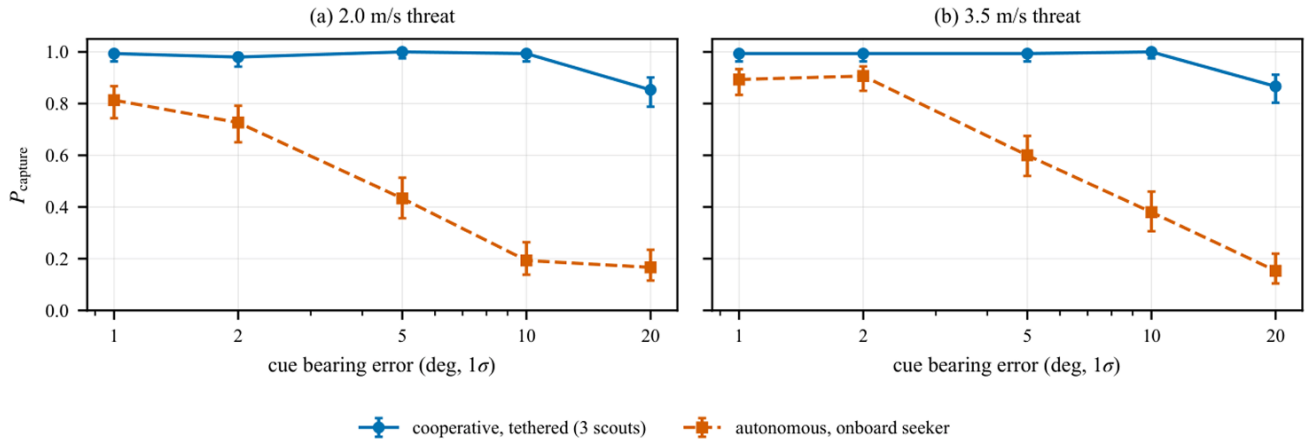


Fig. 5. Cooperative versus cue-fired seeker capture probability versus cue bearing error at 2.0 and 3.5 m/s.

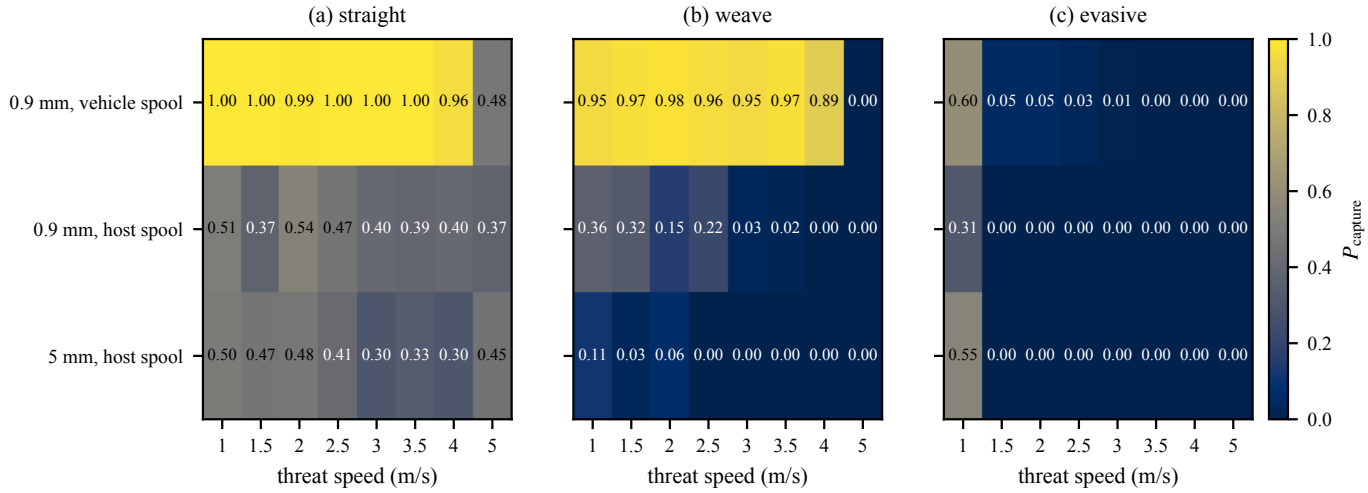


Fig. 6. Capture probability versus threat speed, maneuver, and tether configuration.

clearance envelope rather than contact mechanics, cable sag, or interaction with environmental obstacles.

The sensing and estimation models introduce additional assumptions. Scouts ping independently at the two-way-travel-time limit without mutual sonar interference or receiver blanking; a shared-band implementation would thus reduce revisit rate. Target tracking uses gated nearest-neighbor association, and delayed reports are incorporated at delivery rather than retrodicted. Although the simulator supports multiple targets and decoys, the campaign evaluates only one inbound threat.

Finally, capture is defined geometrically as closest approach within 5 m rather than by a modeled interdiction payload or post-contact outcome. The evasive target follows a deterministic short-horizon turn-away policy rather than an optimized pursuit–evasion strategy, so its low capture rates should not be interpreted as field performance against an optimally maneuvering adversary. Hardware validation is also limited to vehicle integration, tethered bench communications, and fly-by-wire actuation; this paper does not demonstrate open-water target detection, measured tether latency or thrust, or integrated fiber, USBL, sonar, and interdiction performance. These limitations bound the conclusions as architecture-level simulation results rather than validation of an operational counter-UUV system.

IX. Conclusion

KRAKEN demonstrates that counter-UUV interception is not primarily an interceptor-speed problem, but a systems-architecture problem coupling sensing, communications, navigation, and tether mechanics. Cooperative sensing can compensate for uncertain initial cueing, but its advantage depends on maintaining a sufficiently fresh fused track. Likewise, the tether is not merely a communications link: its payout architecture directly constrains vehicle speed, cable interference, and feasible engagement geometry. The resulting design favors distributed scouts, centralized track fusion and guidance, low-latency fiber connectivity, and vehicle-side microcable payout.

These results establish KRAKEN as a candidate architecture rather than an operationally validated counter-UUV system. Future work will integrate fiber, navigation, sonar, multi-vehicle deconfliction, and closed-loop interception in water.

REFERENCES

[1] J. G. Buescher, "A fiber-optic tether for the hull search uuv," United States Navy, SPAWAR Systems Center San Diego, Tech. Rep. Technical Document 3202, Feb. 2006.

[2] Woods Hole Oceanographic Institution, "Nereid ht hybrid rov/auv vehicle," Oct. 2016.

[3] A. D. Bowen *et al.*, "Design of nereid-ui: A remotely operated underwater vehicle for oceanographic access under ice," Woods Hole Oceanographic Institution, Tech. Rep., Aug. 2014.

[4] ——, "Development of a remotely operated underwater vehicle for oceanographic access under ice," in *Proceedings of the 8th Annual Polar Technology Conference*, Apr. 2012.

[5] J. Rosamond, "Plumbing the depths: Unmanned submersibles come of age," ETH Zurich, Center for Security Studies, Tech. Rep., Oct. 2013.

[6] United States Navy, "The navy unmanned undersea vehicle (uuv) master plan," United States Navy, Tech. Rep., Nov. 2004.

[7] N. Boschetti, A. Koyyada, B. Downs, W. Rosenthal, N. Gordon, H. Liwång, A. Marder, J. Sigholm, O. Frånberg, J. Kindgren, T. Frisk, B. M. Magnússon, M. D. Cavelty, H. Johnson, and G. Falco, "Hybrid Space and Submarine Architecture to Ensure Information Security of Telecommunications (HEIST)," *IEEE Access*.

[8] A. Løvik, A. R. Bakken, J. Dybedal, T. Knudsen, and J. Kjøll, "Underwater protection system," in *OCEANS 2007*, 2007.

[9] Y. Pailhas, J. Houssineau, Y. R. Petillot, and D. E. Clark, "Tracking with MIMO sonar systems: Applications to harbour surveillance," *IET Radar, Sonar & Navigation*, vol. 11, no. 4, pp. 629–639, 2017.

[10] E. Simetti, A. Turetta, G. Casalino, and M. Cresta, "Towards the use of a team of USVs for civilian harbour protection: The problem of intercepting detected menaces," in *OCEANS 2010 IEEE Sydney*, 2010.

[11] X. Meng, B. Sun, and D. Zhu, "Harbour protection: Moving invasion target interception for multi-AUV based on prediction planning interception method," *Ocean Engineering*, vol. 219, p. 108268, 2021.

[12] W. Gan and L. Qiao, "Many-versus-many AUV attack-defense game in 3-d scenarios using hierarchical multiagent reinforcement learning," *IEEE Internet of Things Journal*, vol. 12, no. 13, pp. 23 479–23 494, 2025.

[13] A. Bahr, J. J. Leonard, and M. F. Fallon, "Cooperative localization for autonomous underwater vehicles," *The International Journal of Robotics Research*, vol. 28, no. 6, pp. 714–728, 2009.

[14] D. Moreno-Salinas, A. M. Pascoal, and J. Aranda, "Optimal sensor placement for acoustic underwater target positioning with range-only measurements," *IEEE Journal of Oceanic Engineering*, vol. 41, no. 3, pp. 620–643, 2016.

[15] Y. Li, W. Yu, and X. Guan, "Current-aided multiple-AUV cooperative localization and target tracking in anchor-free environments," *IEEE/CAA Journal of Automatica Sinica*, vol. 10, no. 3, pp. 792–806, 2023.

[16] J. Yan, J. Lin, X. Yang, C. Chen, and X. Guan, "Cooperation detection and tracking of underwater target via aerial–surface–underwater vehicles," *IEEE Transactions on Automatic Control*, vol. 70, no. 2, pp. 1068–1083, 2025.

[17] Z. Feng and R. Allen, "Evaluation of the effects of the communication cable on the dynamics of an underwater flight vehicle," *Ocean Engineering*, vol. 31, no. 8–9, pp. 1019–1035, 2004.

[18] M.-C. Fang, C.-S. Hou, and J.-H. Luo, "On the motions of the underwater remotely operated vehicle with the umbilical cable effect," *Ocean Engineering*, vol. 34, no. 8–9, pp. 1275–1289, 2007.

[19] B. Fletcher, C. Young, J. Buescher, L. L. Whitcomb, A. Bowen, R. McCabe, and D. R. Yoerger, "Proof of concept demonstration of the hybrid remotely operated vehicle (HROV) light fiber tether system," in *OCEANS 2008*, 2008.

[20] M. Stojanovic and J. Preisig, "Underwater acoustic communication channels: Propagation models and statistical characterization," *IEEE Communications Magazine*, vol. 47, no. 1, pp. 84–89, 2009.

[21] Z. Li, M. Chitre, and M. Stojanovic, "Underwater acoustic communications," *Nature Reviews Electrical Engineering*, vol. 2, pp. 83–95, 2025.

[22] M. Molins and M. Stojanovic, "Slotted FAMA: A MAC protocol for underwater acoustic networks," in *OCEANS 2006 – Asia Pacific*, 2006, pp. 1–7.

[23] A. A. Syed, W. Ye, and J. S. Heidemann, "T-Lohi: A new class of MAC protocols for underwater acoustic sensor networks," in *IEEE INFOCOM 2008*, 2008, pp. 231–235.

[24] K. B. Kredo, II, P. Djukic, and P. Mohapatra, "STUMP: Exploiting position diversity in the staggered TDMA underwater MAC protocol," in *IEEE INFOCOM 2009*, 2009, pp. 2961–2965.

[25] W. H. Thorp, "Analytic description of the low-frequency attenuation coefficient," *The Journal of the Acoustical Society of America*, vol. 42, no. 1, pp. 270–270, 1967.

[26] R. J. Urick, *Principles of Underwater Sound*, 3rd ed. Los Altos, CA: Peninsula Publishing, 1983.

[27] P. Swerling, "Probability of detection for fluctuating targets," *IRE Transactions on Information Theory*, vol. 6, no. 2, pp. 269–308, 1960.

[28] J. I. Marcum, "A statistical theory of target detection by pulsed radar," *IRE Transactions on Information Theory*, vol. 6, no. 2, pp. 59–267, 1960.

[29] S. M. Kay, *Fundamentals of Statistical Signal Processing, Volume I: Estimation Theory*. Englewood Cliffs, NJ: Prentice Hall, 1993.

[30] P. Zarchan, *Tactical and Strategic Missile Guidance*, 6th ed. Reston, VA: American Institute of Aeronautics and Astronautics, 2012.

[31] E. B. Wilson, "Probable inference, the law of succession, and statistical inference," *Journal of the American Statistical Association*, vol. 22, no. 158, pp. 209–212, 1927.